

# NUCLEAR EMULSION EXPERIMENTS ON PARTICLE PRODUCTION AT HIGH ENERGIES\*

BY I. OTTERLUND

Department of Cosmic High Energy Physics, University of Lund\*\*

(Received September 18, 1976)

Various experimental results, including multiplicities of shower-particles and heavy prong particles, correlations between them and single particle distributions, from proton-emulsion nucleus reactions in the energy range 200 — 400 GeV are presented.

## 1. Introduction

When high energy proton beams became available at Serphukov and at Fermi National Accelerator Laboratory, nuclear emulsion once again appeared as an interesting detector in high energy physics. Since then the interest for emulsion experiments has continued to grow. Recent improvements of the emulsion technique using identifiable nuclear targets may increase the accuracy of the experimental data and stimulate emulsion experiments. Experiments now under way, with emulsion stacks in hybrid systems with electronic tagging, open a new and interesting use of the emulsion technique.

In emulsion experiments the main interest has been to study hadron-nucleus reactions. When the first results on pion multiplicities showed that the intranuclear cascade in the hit nucleus failed to appear at high energies, the experimental and theoretical interest in these problems was immediately quickened.

The main idea was that the nucleus can act as a suitable detector for the space time development of hadron-nucleon reactions, which can hardly be observed in the asymptotic states of produced particles in elementary hadron-nucleon reactions. Now the questions have also been focused on the problems of what really happens when a hadron hits a nucleus. Are there independent reactions between the impinging hadron and target nucleons or does the incident hadron react coherently with several target nucleons? If the latter model is correct, then high energy collisions between particles and nuclei can be used to investigate reactions at very high center of mass energy, using present accelerators [1].

---

\* Presented at the XVI Cracow School of Theoretical Physics, Zakopane, May 25-June 7, 1976.

\*\* University of Lund, Sölvegaten 14, S — 22 3 62 Lund, Sweden.

In this talk I shall present results from emulsion experiments as well as discussing some features of the results which are of importance for our understanding of hadron-nucleus reactions.

First, I shall make a few comments on the notations used in proton-nucleus experiments with the emulsion technique. Then, I shall summarize the multiplicity data obtained in proton-emulsion nucleus reactions in the energy range 200–400 GeV. I shall briefly discuss new methods of emulsion techniques where the targets are embedded in the emulsion. I shall give a thorough discussion of the angular distributions, and, finally, I shall compare the experimental results with the predictions from *independent particle models* and *collective ones*.

## 2. Notations in proton-emulsion nucleus experiments

In the study of hadron-emulsion nucleus interactions, the nuclear emulsion is in general used as both target and detector. The targets consist of hydrogen, a light (L) group of CNO-targets and a heavy (H) group of AgBr-targets.

The mean mass of emulsion nuclei is 60 [2]. The light nuclei have a mean mass equal to 14; and the heavy nuclei have a mean mass equal to 94.

The incident proton interacts in 5% with H, in 25% with CNO and in 70% with AgBr.

The average number of encounters between an incident hadron and the nucleons in the target nucleus is denoted  $\bar{v}$ .  $\bar{v}$  is defined from the equation

$$\bar{v} = \frac{A\sigma_{hp}}{\sigma_{hA}}, \quad (1)$$

where  $\sigma_{hp}$  and  $\sigma_{hA}$  are the inelastic cross-sections for hadron-proton and hadron-nucleus interactions [2, 3]. Experimental values of the inelastic cross-sections give [4]

$$\pi\text{-}A \text{ interactions } \bar{v} = 0.74 A^{0.25}, \quad (2)$$

$$p\text{-}A \text{ interactions } \bar{v} = 0.70 A^{0.31}.$$

For proton-emulsion nucleus reactions, it follows that  $\bar{v}_L = 1.6$  and  $\bar{v}_H = 2.9$ .

It is interesting to note that in about 40% of the interactions observed in the emulsions the impinging proton has only made one encounter with the target nucleons. The probability  $\pi(1)$  that there will be only one collision when a proton of energy  $E_0$  impinges upon emulsion nuclei has been estimated to be [5]

$$\pi(1)_L = 0.58 \quad \text{and} \quad \pi(1)_H = 0.29. \quad (3)$$

The particles emitted in the interactions are classified according to the ionization produced along the tracks. Normally, we do not identify the particles. Consequently, we simply call them black, grey and heavy track-producing particles and shower-particles.

$n_b$  — the number of *black track-producing particles*. These particles have an ionization of  $I > 6.8 I_0$ , where  $I_0$  is the ionization of the primary proton. This ionization range

corresponds to protons with energies  $\lesssim 30$  MeV. Black track-producing particles are mainly fragments emitted from the excited target. They have energy and angular distributions typical of thermal processes;

$n_g$  — the number of *grey track-producing particles*. The ionization of these tracks are  $6.8 I_0 > I > 1.4 I_0$ , corresponding to protons in the energy range 30–400 MeV. Grey track-particles are believed to be associated with the recoiling particles. In reactions with light nuclei  $\langle n_g \rangle_L \approx 0.6 \bar{v}$ , and in reactions with heavy nuclei  $\langle n_g \rangle_H \approx 1.1 \bar{v}$  [6]. Thus  $\langle n_g \rangle_A$  increases faster than  $\bar{v}_A$  with the target mass. It has been established that  $\langle n_g \rangle_A \sim A^{2/3}$  [6];

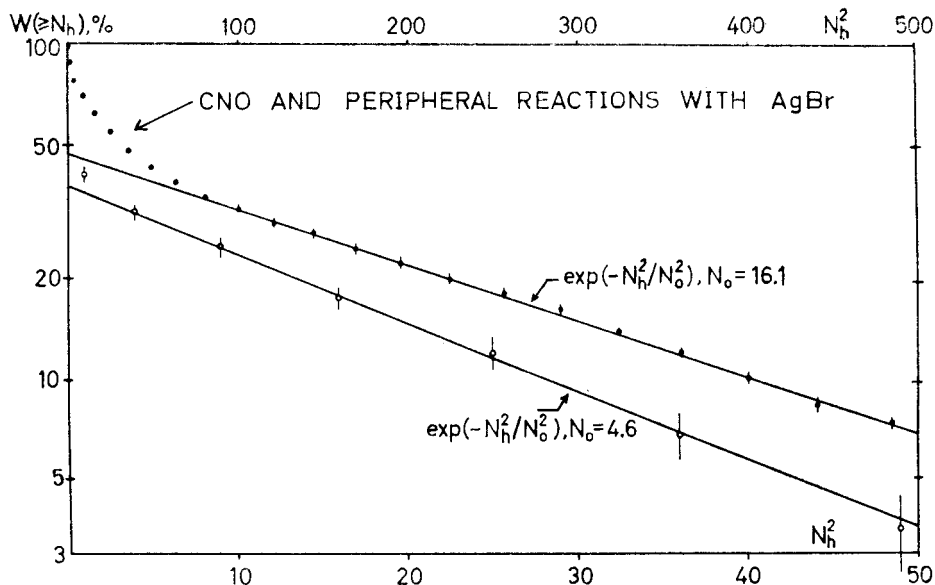


Fig. 1. Integral  $N_h$ -distribution for all events — (a) and for events remaining after subtraction of Eq. (4) — (b) (Ref. [6])

$N_h = n_g + n_b$  = the number of *heavy prong particles* (having  $\beta < 0.7$ ).  $N_h$  is interpreted as the number of charged fragments emitted from the target.  $\langle N_h \rangle_{pA}$  seems to be energy-independent but depends on the target mass as  $\sim A^{2/3}$  [6]. It has been found that  $\langle N_h \rangle_L \approx 1.7 \bar{v}$  and  $\langle N_h \rangle_H \approx 3.3 \bar{v}$ .

Figure 1 shows the integral  $N_h$ -distribution as a function of  $N_h^2$ , estimated by the Alma-Ata-Leningrad-Moscow-Tashkent collaboration [6]. These scientists found that in the range  $N_h \geq 8$  the integral probability distribution  $W(\geq N_h)$  vs  $N_h^2$  is well consistent with the exponential function

$$W(\geq N_h) \sim \exp(-N_h^2/N_0^2), \quad N_0 = 16.1. \quad (4)$$

About 37% of the proton-nucleus interactions have  $N_h \geq 8$ , and thus about 47% of the interactions with AgBr have  $N_h < 8$ . These reactions, with a small number of heavy prongs, are difficult to distinguish from reactions with CNO.

The difference between the experimental distribution for  $N_h \geq 2$  and the distribution given by Eq. (4) is also in fairly good agreement with equation (4) but with  $N_0 = 4.6$ . (See Fig. 1 and Ref. [6]).

If Eq. (4) describes collisions with the core of heavy nuclei, where the density of nuclear matter is uniform, then the exponential function with  $N_0 = 4.6$  may describe the peripheral region of the target with decreasing nuclear density, this region being rather independent of the nuclear size [6]. These assumptions have been used in order statistically to separate reactions with CNO from reaction with AgBr [6-9].

$n_s$  — the number of shower-particles. These particles have  $\beta \geq 0.7$  ( $I \leq 1.4 I_0$ );

$\langle n_s \rangle_A$  — the average number of shower-particles produced in an inelastic reaction between a hadron and a nucleus  $A$ . It is well established that  $\langle n_s \rangle_A$  has a very weak mass dependence  $\sim A^{0.13}$  [10];

$\langle n_{ch} \rangle$  — the average number of charged particles observed in a collision of a hadron with a proton;

$\langle n_s \rangle_1$  — the average number of shower-particles produced in a hadron-nucleon collision. This multiplicity is approximately given by the equation [11]:

$$\langle n_s \rangle_1 = \langle n_{ch} \rangle - 0.5. \quad (5)$$

The quantity  $R = \frac{\langle n_s \rangle_A}{\langle n_{ch} \rangle}$ , which is a measurement of the shower-particle multiplicity in hadron-nucleus reactions to the charged-particle multiplicity in hadron-proton reactions, has frequently been used for the interpretation of the data. It is found that  $R$  is energy-dependent for  $E_0 < 60$  GeV but has a very weak dependence on energy when  $E_0 \gtrsim 60$  GeV [12]. However, the multiplicity  $\langle n_{ch} \rangle$ , obtained in pp reactions, is not the relevant parameter in connection with the experimental observables in proton-emulsion nucleus interactions. The reason is that  $\langle n_{ch} \rangle$  contains all charged secondaries whereas the charged-particle multiplicity obtained in emulsion is partitioned into two parts: the *shower-particle multiplicity* and the *heavy prong particle multiplicity*. The number of fast recoiling protons from the target, identified as shower-particles, is not very well known. Loos et al. [13] found, for example, in  $\pi$ -Ne collisions that the events of high multiplicity include energetic protons with momenta above 1 GeV/c in the laboratory. These events probably arise from multiple nuclear collision processes within the Ne nucleus. A knowledge of the amount as well as the angular and energy distributions of the fast knock-out target protons is evidently essential to a correct interpretation of the experimental data and to an understanding of the reaction mechanisms. Many suggestions as to how to estimate  $R$ , taking into account the admixture of target protons, have been brought forward.

A related quantity  $R_{eq}$  for the interpretation of the data is defined by the relation (the index "eq" stands for equivalent [5]):

$$R_{eq} = \frac{\langle n_s \rangle_A}{\langle n_s \rangle_1}. \quad (6)$$

In Fig. 2,  $R_{eq}$  is shown as a function of energy.

Babecki [14] has recently introduced the mean normalized multiplicity  $R_1$ . He suggests that if  $\langle n_{\text{ch}} \rangle$  is used for comparison, one should correct for the missing slow particles, which are not included in  $\langle n_s \rangle$ . The total mean multiplicity of charged particles in the interactions of protons with nuclei of a mass number  $A$  is then [14].

$$\langle n \rangle_A = \langle n_s \rangle_A + \bar{\nu}_A(n_\pi + l_p n_p), \quad (7)$$

$\bar{\nu}_A$  — the mean number of collisions in the target nucleus,  $l_p$  — the fraction of protons among the nucleons of nucleus  $A$  ( $l_p \approx 0.455$ ),  $n_p$  — the mean number of slow protons ( $n_p \approx 0.48$  from Ref. [11]),  $n_\pi$  — the mean number of slow pions ( $n_\pi \approx 0.14$  from Ref. [11]).

$$R_1 = \frac{\langle n \rangle}{\langle n_{\text{ch}} \rangle} = R_A + \frac{\delta}{\langle n_{\text{ch}} \rangle}. \quad (8)$$

At 200 GeV, there is an approximately 7% difference between  $R_1$  and  $R_A = \frac{\langle n_s \rangle}{\langle n_{\text{ch}} \rangle}$ .

Babecki [14] also discusses the normalized multiplicity of “created” particles  $R_2$  or better created charges in a reaction. He only counts the number of charges which have been cre-

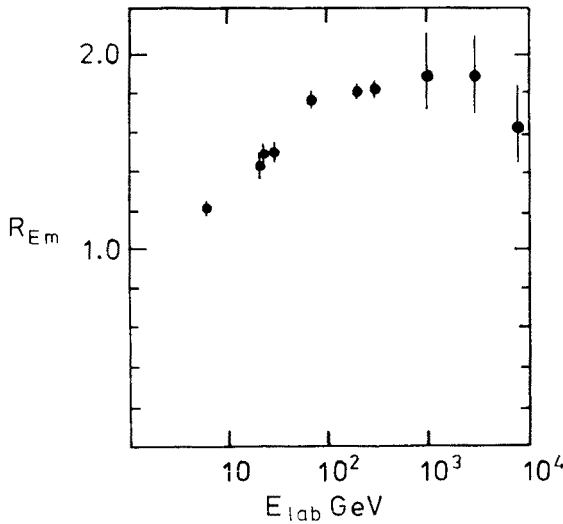


Fig. 2.  $R_{\text{eq}} = \frac{\langle n_s \rangle}{\langle n_s \rangle_1}$  as a function of energy [2]

ated in the reaction. In a proton-proton collision, there are two charges before the reaction, and consequently  $\langle n \rangle_H - 2$  charges are created during the reaction. If the incident proton collides with  $\bar{\nu}$  nucleons in the target, we expect, on an average, that  $\bar{\nu}l_p$  nucleons are protons. Thus, there are  $1 + \bar{\nu}l_p$  charges in the initial state. In the final state,  $\langle n \rangle - (1 + \bar{\nu}l_p)$  created-charges are observed.

$$R_2 = \frac{\langle n \rangle - (1 + \bar{\nu}l_p)}{\langle n_{\text{ch}} \rangle - 2}. \quad (9)$$

Figure 3 shows  $R_2$  as a function of energy. It is evident that  $R_2$  does not depend on energy. Thus, the growth in  $R$  with energy depends on the fact that  $\langle n_{ch} \rangle$  contains all secondaries whereas  $n_s$  does not include all the recoiling protons.

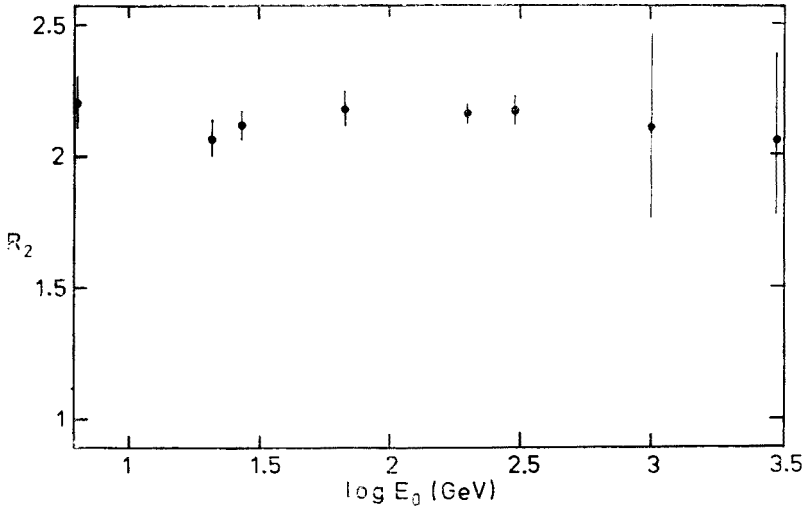


Fig. 3.  $R_2$  as a function of  $E_0$  for emulsion nucleus interactions (Ref. [14])

In emulsion experiments on multiparticle production, emission angles  $\theta$  are measured. From these measurements it is possible to obtain rapidity distributions by the use of the pseudorapidity variable:

$$Y_{lab} \approx \eta = -\ln \operatorname{tg} \theta/2. \quad (10)$$

A comparison between  $Y_{lab}$  and  $\eta$  is given, for example, in Ref. [2].

### 3. Multiplicities in interactions of 200–400 GeV protons in emulsion<sup>1</sup>

#### 3.1. Multiplicity distributions

Some characteristics of the multiplicity distributions at 200–400 GeV are given in Table I. The 400 GeV results are preliminary, being based on only 468 reactions [15]. The average shower-particle multiplicity in events  $N_h = 0$  and 1, after subtracting contributions due to hydrogen in emulsion and coherent reactions, is at 200 GeV  $9.2 \pm 0.4$  and at 300 GeV  $10.5 \pm 0.6$ . This is much larger than the shower-particle multiplicity  $\langle n_s \rangle_1$

<sup>1</sup> Chapters 3 and 6 are based on work obtained in collaboration with: M. Juric and O. Adamovic, Univ. of Belgrade, Belgrade, Yugoslavia; B. Andersson and R. Haglund, Univ. of Lund, Lund, Sweden; G. Bauman and R. Devienne, Univ. of Nancy, Nancy, France; H. Areti, C. J. D. Hebert and J. Hebert, Univ. of Ottawa, Ottawa, Canada; J. Long, C. Meton, D. Schune, Tsai-Chü and B. Willot, LPNHE, Université Pierre et Marie Curie, Paris, France; G. Baroni, S. Di Liberto, F. Meddi, S. Petrera and G. Romano, Istituto Nazionale di Fisica Nucleare, Roma, Italy; J. M. Bolta and G. Rey, Instituto de Fisica Corpuscular, Valencia, Spain.

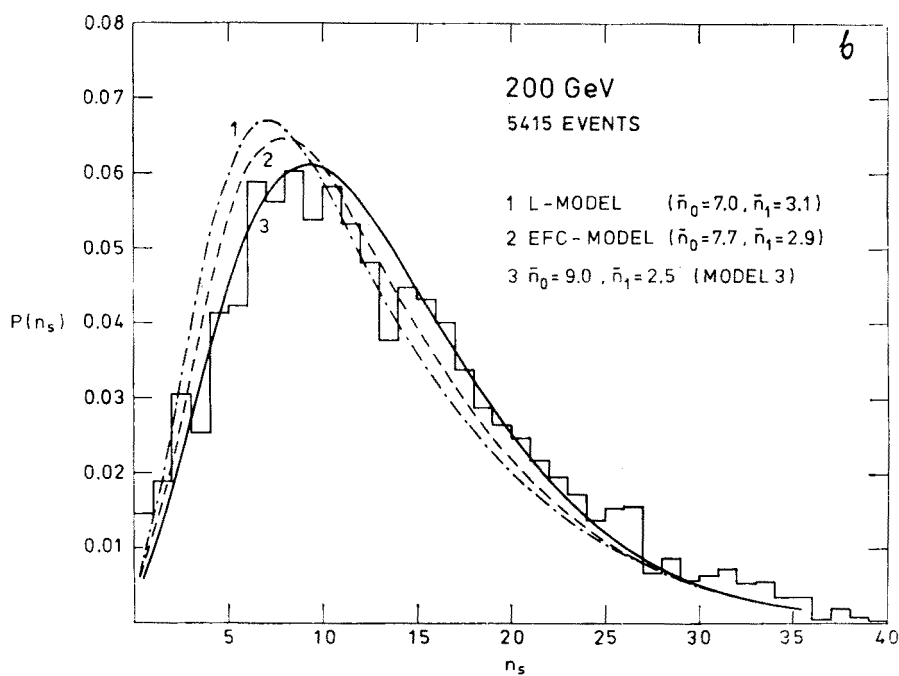
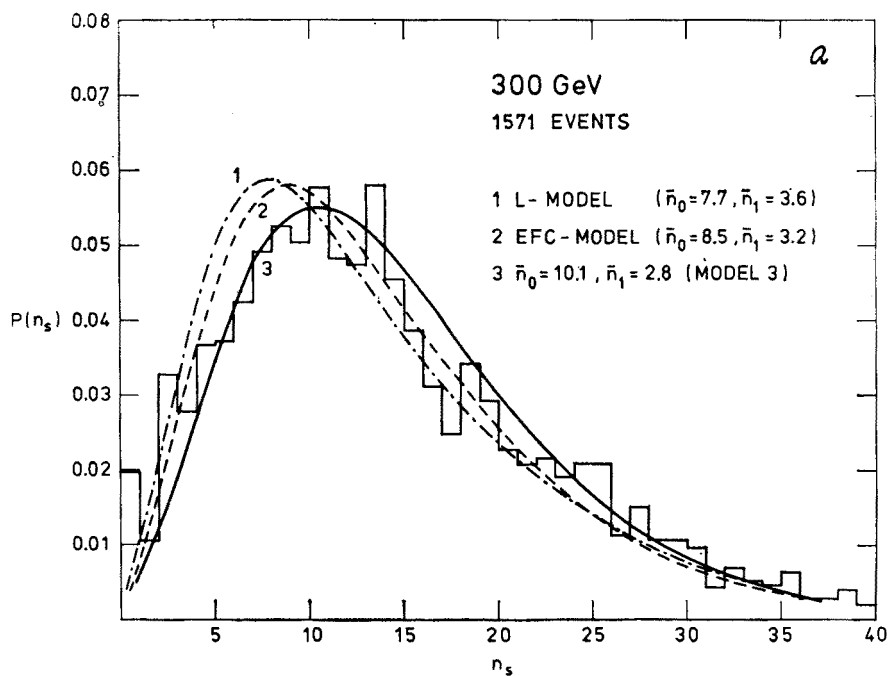


Fig. 4. Shower-particle multiplicity distributions. The curves show theoretical distributions for three models discussed in the text and in Ref. [5]: a) 300 GeV, b) 200 GeV

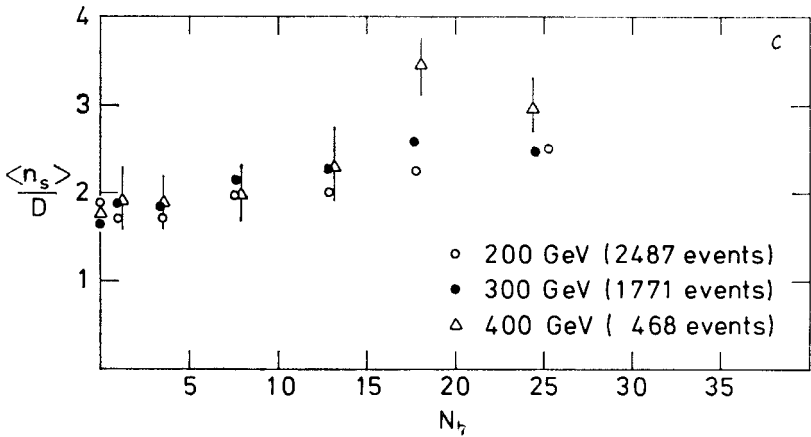
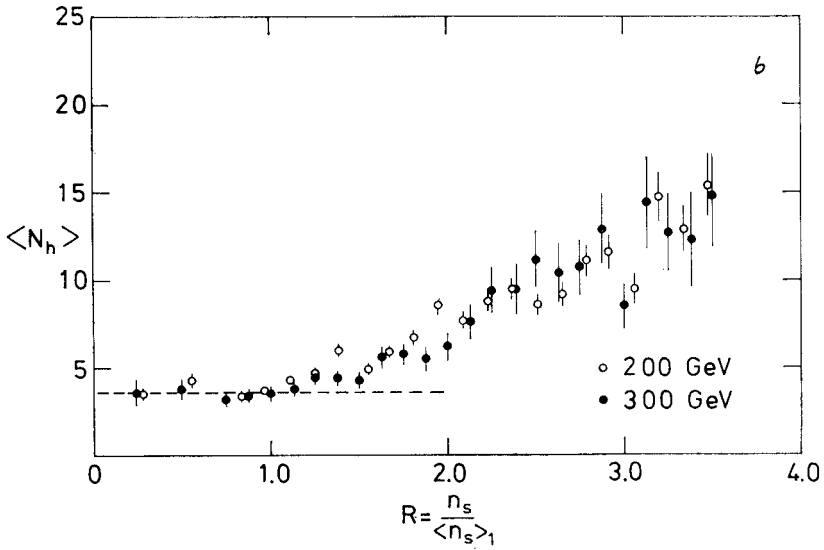
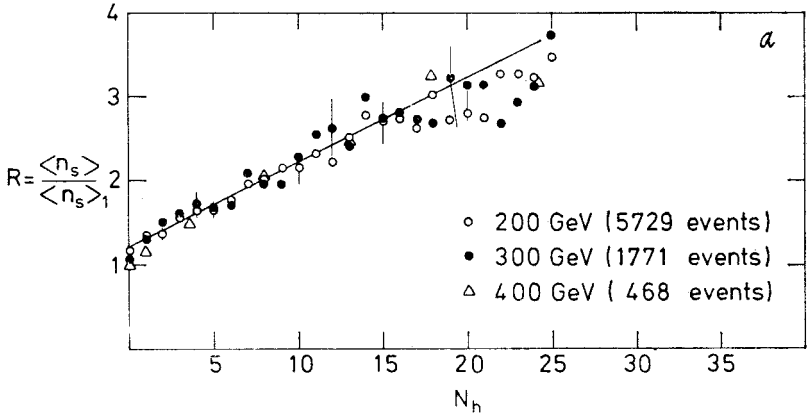




TABLE I

Characteristics of the multiplicity distributions

| Energy(GeV) | $\langle n_s \rangle_{Em}$ | $\langle n_s \rangle_{CNO}$ | $\langle R \rangle_{CNO}$ | $\langle n_s \rangle_{AgBr}$ | $\langle R \rangle_{AgBr}$ | $\langle n_s \rangle/D$ | $\langle N_h \rangle$ |
|-------------|----------------------------|-----------------------------|---------------------------|------------------------------|----------------------------|-------------------------|-----------------------|
| 200         | $13.2 \pm 0.2$             | $10.9 \pm 0.3$              | $1.42 \pm 0.04$           | $15.1 \pm 0.3$               | $1.97 \pm 0.05$            | $1.66 \pm 0.08$         | $7.4 \pm 0.1$         |
| 300         | $15.1 \pm 0.2$             | $12.1 \pm 0.5$              | $1.42 \pm 0.07$           | $16.7 \pm 0.5$               | $1.96 \pm 0.06$            | $1.68 \pm 0.04$         | $7.2 \pm 0.1$         |
| 400         | $16.3 \pm 0.4$             |                             |                           |                              |                            |                         | $7.9 \pm 0.4$         |

$= 7.18 \pm 0.12$ , respectively  $\langle n_s \rangle_1 = 8.0 \pm 0.2$ , observed in proton-nucleon reactions at 200 and 300 GeV [16]. The mean multiplicity in light and heavy emulsion nuclei at 200 GeV has been estimated, using a method introduced by Florian et al. [7]. It is evident that the mean value of the ratios  $\langle R \rangle_{CNO}$  and  $\langle R \rangle_{AgBr}$ , the ratio of the mean and the dispersion of the shower-particle distribution  $\langle n_s \rangle/D$  as well as the mean number of heavy prongs  $\langle N_h \rangle$ , change little from 200 GeV to 300 GeV.

Multiplicity distributions at 200 and 300 GeV are shown in Figs 4a and b [5, 6, 8, 18, 19].

### 3.2. Correlations between shower-particles and heavy prongs

In Figs 5a, b and c, we exhibit some features of the correlations between the shower-particle distribution and the heavy prong distribution, and compare the data at 200 GeV, 300 GeV and 400 GeV [15]. In Fig. 5a, the mean value of  $R$  is plotted for different values of  $N_h$ . In Fig. 5b, the mean value of  $N_h$  is plotted for different values of  $R$ . In Fig. 5c the ratio  $\langle n_s \rangle/D$  for the shower-particle multiplicity is shown as a function of  $N_h$ .

From Figs 5a-c we conclude that the features of the 200, 300 and 400 GeV data are very similar. In particular, the close correlation between projectile fragmentation (i. e. the shower particles) and target fragmentation (i. e. heavy prongs) is noticeable. There seems to be an obvious difference between reactions with  $v = 1$ , and those with  $v > 1$ . We can see the difference in the constancy of  $\langle N_h \rangle$  for values of  $R < 1$ , and the increase of  $\langle N_h \rangle$  for  $R > 1$ . The increase in  $\langle N_h \rangle$  for  $R > 1$  can be understood in terms of inelastic repeated collisions inside the nucleus [5]. The small variation of  $\langle n_s \rangle/D$  with  $N_h$  seems to indicate that such collisions are not easily treated as independent [20].

### 3.3. Shower-particles emitted backwards in the laboratory system

The Kobe-Osaka collaboration has pointed out that the shower-particles emitted in the backward hemisphere in the laboratory system are remarkably abundant [21]. This is shown in Fig. 6, where the number of shower-particles in the backward direction

Fig. 5. a)  $R_{eq} = \frac{\langle n_s \rangle}{\langle n_{ch} \rangle - 0.5}$  as a function of  $N_h$  (Ref. [15]), b)  $\langle N_h \rangle$  as a function of  $R_{eq}$  (Ref. [15]),

c)  $\frac{\langle n_s \rangle}{D}$  as a function of  $N_h$  (Ref. [15])

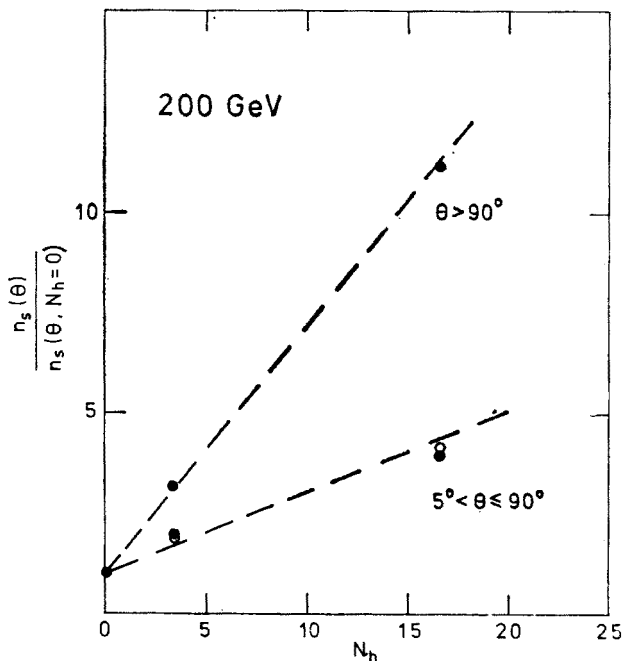


Fig. 6. The number of shower-particles in the backward direction and in the angular interval  $5^\circ < \theta \leq 90^\circ$ . The values are normalized to 1 at  $N_h = 0$ . Full circles from Ref. [21] open circles from Ref. [8]

and in the angular interval  $5^\circ < \theta \leq 90^\circ$  are compared. It is evident that the frequency of backward tracks increases with  $N_h$  much more strongly than that of average multiplicity of shower-particles in the angular interval  $5^\circ$ – $90^\circ$ .

#### 4. Studies of hadron-nucleus interactions using nuclear emulsion with embedded targets

Despite the many favourable features nuclear emulsions offer to physicists, there are also a few disadvantages. The most conspicuous one of these is intrinsic to their nature as an inhomogeneous medium, denoted by the great variety of nuclei in the emulsion. Consequently, when the emulsions are used to study the interactions of incoming particles with the nuclei of the emulsions, it is not possible to determine the identity of the nucleus involved with any degree of certainty.

One method used for the study in emulsions of the events produced in an element has been to load emulsions with wires. The first incorporation of wires into nuclear emulsions was described by Occhialini et al. [22] and Danysz and Yekutieli [23]. The most important problem they encountered in processing such plates was the elimination of the distortion introduced by the presence of the wires. This arises from volume changes of the emulsion and movements of the wires during the processing.

A new method of introducing known targets into nuclear emulsions has been developed by B. Lindkvist [24]. In this method, fine wires are embedded in the median plane of

nuclear emulsions. Fig. 7 shows a nuclear emulsion with embedded wires. Two emulsions — one stripped emulsion and one emulsion on glass — are laminated with fine wires in a grid between the emulsions. The method makes it possible to develop the emulsions without any distortion.

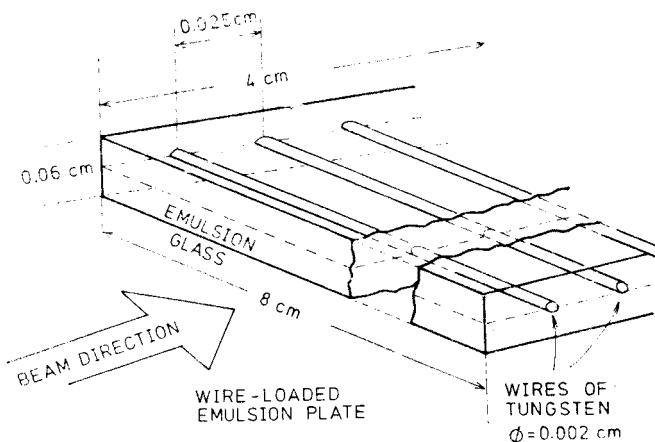


Fig. 7. Nuclear emulsions with embedded wires (Ref. [24])

Another method has been used by Lord et al. [25]. A mixture of one gram of powder and about 100 cc of water was poured quickly over a 200  $\mu\text{m}$  emulsion on glass. A second 200 micron emulsion layer was finally added and the resultant sandwich was dried. The average granule diameter in their loaded emulsions is about 15 microns.

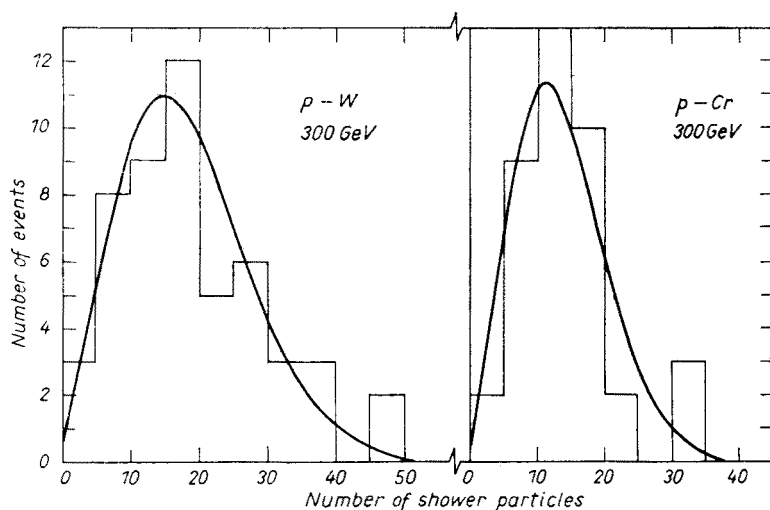


Fig. 8. Shower-particle multiplicity distributions for tungsten and chromium. The solid curves are obtained by a KNO-like scaling of the charged multiplicity distribution in proton-proton interactions (Ref. [25])

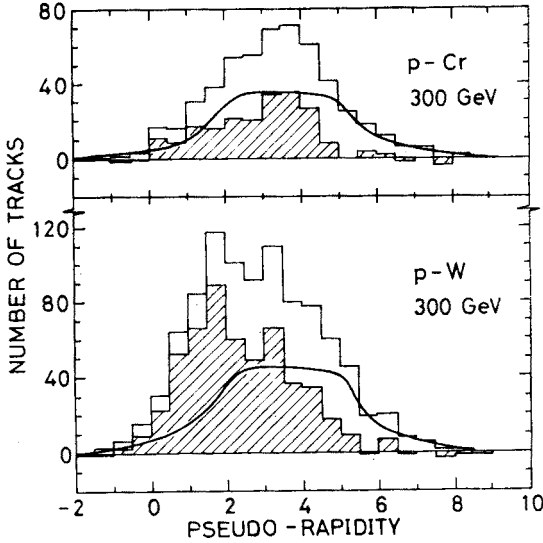


Fig. 9. Pseudo-rapidity distributions for the chromium and tungsten events. The solid curve represents hydrogen data. Also shown are the “excess” pseudo-rapidity distribution for tungsten and chromium obtained by subtracting the p–p distribution (the shaded histogram) (Ref. [25])

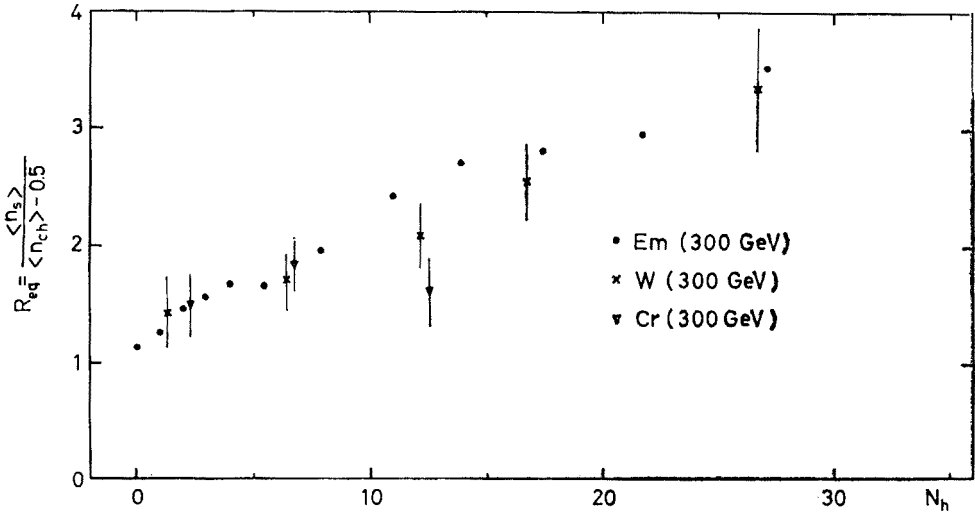


Fig. 10.  $R_{eq}$  as a function of  $N_h$

Figures 8, 9 and 10 show results obtained with the technique of loaded emulsions. Figs 8 and 9 show shower-particle multiplicity distributions and rapidity distributions for p–W and p–Cr reactions obtained by Florian et al. [25]. Fig. 10 shows

$$R_{eq} = \frac{\langle n_s \rangle}{\langle n_{ch} \rangle - 0.5}$$

as a function of  $N_h$ .

The black points show the emulsion data of 300 GeV [15]. The triangles are from p-Cr reactions [25]. The consequence of the limited size of the target is obvious. When the number of heavy prongs approaches the number of protons in the hit nucleus, the linear correlation between  $R$  and  $N_h$  disappears [25, 26].

Data from p-W reactions obtained by Florian et al. [25] are also shown in Fig. 10. The p-W results are similar to the emulsion results and they also show a slightly linear behaviour. We conclude that the correlation between  $R$  and  $N_h$  is not only energy-independent but also seems to be comparatively independent of the target mass, at least when  $N_h \ll Z$  [25].

### 5. A comparison of the angular distributions in p-nucleus and pp interactions

In several previous papers describing the very forward particles, it has been observed that the angular distributions does not depend on the size of the target and agree with the pp distributions. As an example, distributions obtained by the Alma-Ata-Leningrad-Moscow-Tashkent collaboration are shown in Fig. 11 [27]. No difference in the angular distributions in proton-nucleus and proton-proton reactions is seen for  $n_s \leq 8$  and  $9 \leq n_s \leq 16$  whereas the  $A$ -dependence for  $n_s \geq 17$  is very marked for large angles.

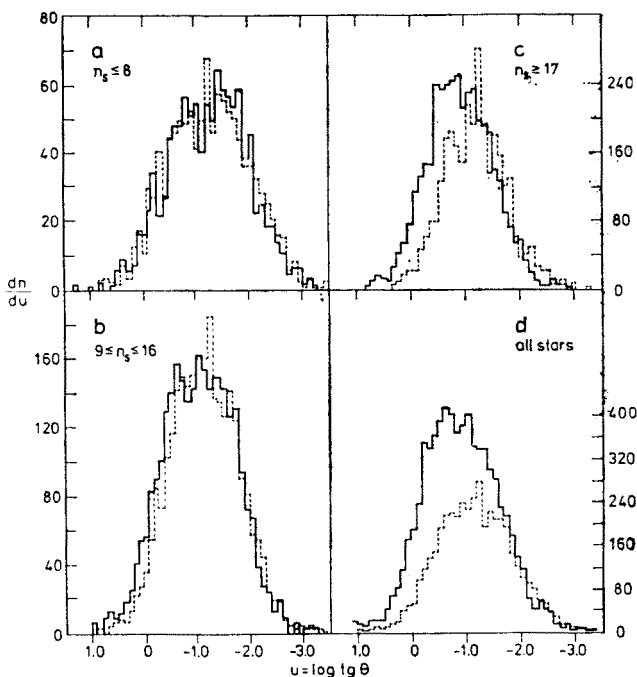


Fig. 11. Angular distributions of shower-particles for interactions with different  $n_s$ : a)  $n_s \leq 8$ , b)  $9 \leq n_s \leq 16$ , c)  $n_s \geq 17$ , d) summary distribution of all stars (without proton-nucleon and coherent reactions). Solid line — proton-nucleus interactions, dashed line — pp interactions. The normalization is to the number of interactions (Ref. [27])

The Alma-Ata-Leningrad-Moscow-Tashkent collaboration [27] have also compared the multiplicities of relativistic particles in p-nucleus and pp-reactions in different rapidity regions. They found that:

|                                       |                   |
|---------------------------------------|-------------------|
| $R$ (target fragmentation region)     | $= 2.72 \pm 0.15$ |
| $R$ (pionization region)              | $= 1.46 \pm 0.09$ |
| $R$ (projectile fragmentation region) | $= 0.82 \pm 0.06$ |

Thus, the excess of particles is in the pionization and in the target fragmentation regions whereas a deficit of particles is observed in the projectile fragmentation region.

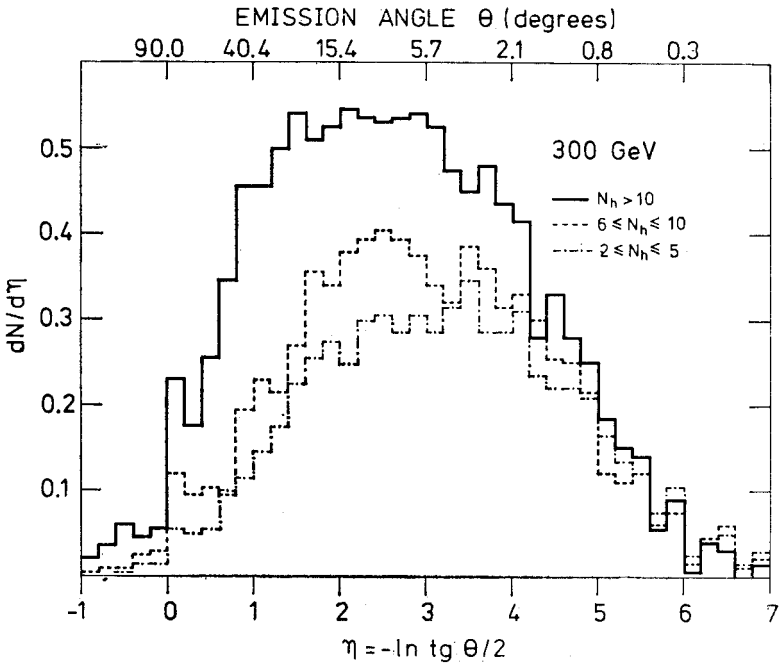


Fig. 12. Angular distributions in different  $N_h$  intervals (Ref. [15])

The change of the angular distribution with  $N_h$  is shown in Fig. 12 for p-nucleus reactions at 300 GeV [15]. The excess of produced particles depends on  $N_h$ , and is observed in the target fragmentation region and in the pionization region.

6. Rapidity distributions

The pseudorapidity distributions of shower-particles are plotted in Figs 13a-c for different star sizes [15]. The most salient features are the following:

- The  $\eta$ -distributions at 200 and 300 GeV are (for fixed  $N_h$ ) essentially the same in the target fragmentation region.

TABLE IIa

Shower particle multiplicities in the pseudorapidity region  $\eta < 3.0$  ( $\theta > 5^\circ.7$ )

| $N_h$ -range | $\langle n_s \rangle$ |                |
|--------------|-----------------------|----------------|
|              | 300 GeV               | 200 GeV        |
| 2 — 5        | $5.9 \pm 0.3$         | $5.8 \pm 0.4$  |
| 6 — 10       | $8.0 \pm 0.6$         | $8.0 \pm 0.7$  |
| > 10         | $13.7 \pm 0.8$        | $13.6 \pm 1.0$ |

TABLE IIb

Shower particle multiplicity in the pseudorapidity region  $\eta > 3.0$  ( $\theta < 5^\circ.7$ )

| $N_h$ -range | $\langle n_s \rangle$ |               |
|--------------|-----------------------|---------------|
|              | 300 GeV               | 200 GeV       |
| 2 — 5        | $7.0 \pm 0.4$         | $4.8 \pm 0.3$ |
| 6 — 10       | $7.8 \pm 0.6$         | $5.7 \pm 0.5$ |
| > 10         | $9.5 \pm 0.5$         | $6.3 \pm 0.4$ |

This effect can be made evident by an investigation of the number of shower-particles emitted in the direction  $\eta < \eta_b$ . In Table IIa, we exhibit the numbers obtained for  $\eta_b = 3.0$  for different  $N_h$ -ranges. Similar results are obtained for  $\eta_b < 3.0$ . (The value  $\eta = 3.0$  is, if the transverse momentum distribution is the same for proton-proton and proton-nucleus interactions, close to  $y_{\text{CMS}}$  for 200 GeV.)

- The number of shower-particles emitted in the direction  $\eta > \eta_t$  greatly increases with energy. In Table IIb, this effect is exhibited for  $\eta_t = 3.0$  for different  $N_h$ -energies, similar results being also obtained for  $\eta_t > 3.0$ .
- The widths of the distributions at 300 GeV are always larger than the widths at 200 GeV.
- The angular distributions are similar to pp-distributions for angles  $\theta < \theta_c$ , but it seems that  $\theta_c$  is energy-dependent (decreasing with energy).

A related rapidity distribution is the integral distribution  $n_s(\eta, N_h)$ , defined as the total number of shower particles with angles smaller than the one characterized by the parameter  $\eta = -\ln \tan \theta/2$  in events corresponding to a fixed number  $N_h$  of heavy prongs.

Fig. 14a shows  $n_s(\eta, N_h)$  for fixed values of the parameter  $\eta$ . There is evidently a linear dependence on the number of heavy prongs. We define the two functions  $\alpha(\eta)$  and  $\beta(\eta)$  by means of the relationship

$$n_s(\eta, N_h) = \alpha(\eta) + \beta(\eta) \cdot N_h. \quad (11)$$

For small angles the number of shower-particles  $n_s(\eta, N_h)$  seems to be rather insensitive to an increasing path length of the leading particle in nuclear matter ( $N_h$ ) (we interpret  $N_h$  as a probe for the number of target nucleons participating in a reaction).

In the actual construction of the two functions  $\alpha$  and  $\beta$ , we have made use of events corresponding to  $2 \leq N_h < 20$ . We use this  $N_h$  interval since the linear relationship

does not seem to be valid for  $N_h \geq 20$ , and events with  $N_h = 0$  and 1 contain coherent reactions and pp collisions.

Figure 13 exhibits the results of such a construction of  $\alpha(\eta)$  and  $\beta(\eta)$  for 200 GeV and 300 GeV. It is evident that at angles with  $\eta = \sim 4.3$  ( $1.6^\circ$ ) for  $E_0 = 200$  GeV, and

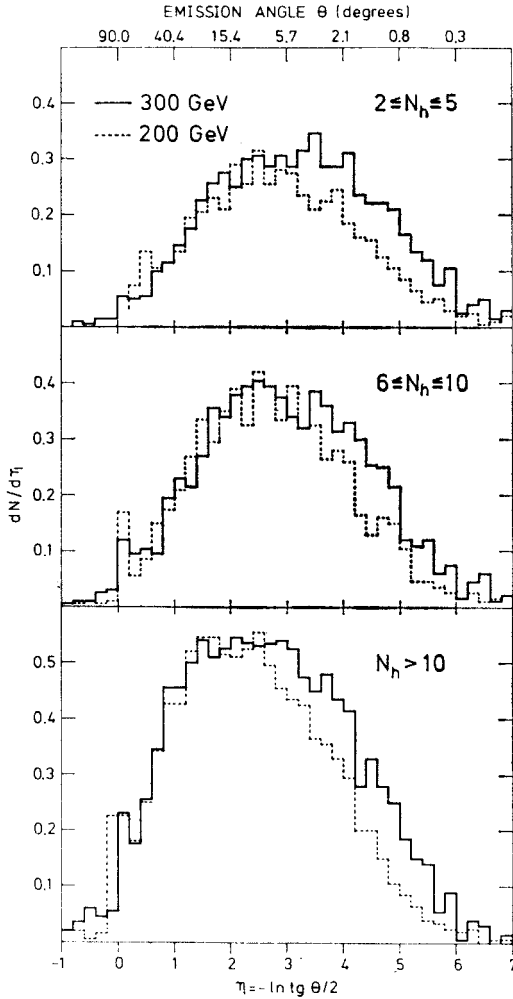


Fig. 13. Pseudo-rapidity distributions of shower-particles for three different star sizes and two different incident energies

for angles with  $\eta \sim 5$  ( $0.8^\circ$ ) for  $E_0 = 300$  GeV, there are already correlations to the nuclear parameters, i.e. the function  $\beta(\eta)$  is non-vanishing [15].

The coefficients  $\alpha(\eta)$  and  $\beta(\eta)$  may be interpreted such that the differential distributions  $d\alpha/d\eta$  mainly describes the angular distribution of shower particles from the leading particle, while  $d\beta/d\eta$  describes the angular distribution of pions emitted in repeated collisions.



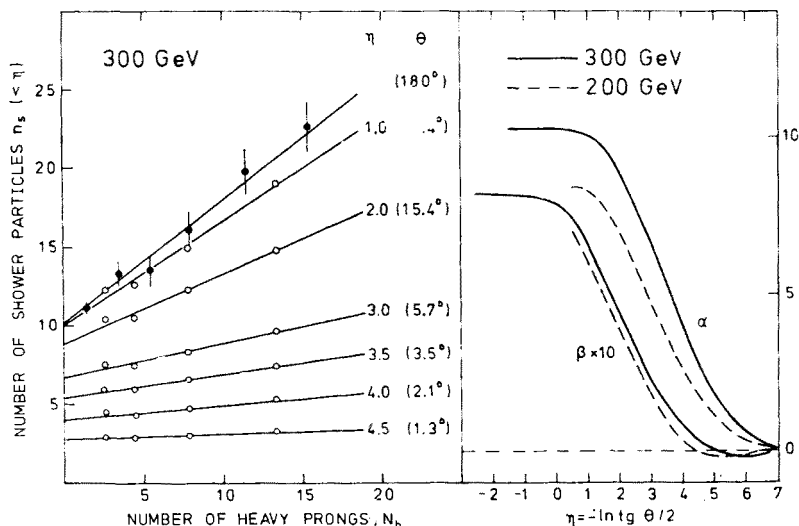


Fig. 14. a)  $n_s(\eta, N_h)$  as a function of  $N_h$ , b)  $\alpha$  and  $\beta$  as a function of  $\eta = -\ln \lg \theta/2$  (Ref. [15])

It is evident that  $\beta(\eta)$  has a similar slope at 300 and 200 GeV. On the other hand,  $\alpha(\eta)$  has different slopes at 300 and 200 GeV. This means that the differential distributions  $d\beta/d\eta$  will be comparatively similar at 300 and 200 GeV whereas  $dx/d\eta$  will be strongly different.

## 7. Models for hadron-nucleus collisions

### 7.1.

A number of ideas and models have been discussed in connection with proton-nucleus experimental findings [28–37]; hydrodynamical models [29], multiperipheral models [30], non interacting fireballs [31], energy flux cascade models [32], the noeva cascade model [33], the coherent production model [34], the coherent tube model [1] and so forth. In this talk I shall only discuss collective models and independent particle models as well as making some comparisons between experimental results and the predictions ensuing from these models.

### 7.2. Collective models

In collective models, one assumes that in a high-energy hadron-nucleus reaction the nucleons in the path of the incident hadron inside the target nucleus can be viewed as acting collectively and in the first order approximation be considered as a single object [1, 36, 37].

When a high energy particle with laboratory energy  $E_0$  collides with a target nucleon at rest, the centre of mass energy squared,  $s$ , is given approximately by

$$s \approx 2mE_0 \quad (12)$$

where  $m$  is the nucleon mass.

If the incident hadron interacts with  $i$  nucleons simultaneously, the centre of mass energy squared is

$$s_{\text{eff}} \cong 2imE_0 \cong i \cdot s. \quad (13)$$

The *Coherent Tube Model* suggested by Dar et al. [1] is based on two simple assumptions, namely that:

- The interactions of a high energy particle with a target nucleus result from its simultaneous collision with all the nucleons that lie within a tube of cross section  $\sigma$  along its path in the target nucleus.
- In the centre of mass system, the particle-tube collision resembles a particle-nucleon collision at the same centre of mass energy.

The Coherent Tube Model predicts that

$$\langle n_s(s) \rangle_A \cong \langle n_s(s_{\text{eff}}) \rangle_p. \quad (14)$$

If one assumes that the relativistic-charged particle multiplicity in particle-nucleon collisions increases as

$$\langle n(s) \rangle_p \cong \langle n(s_0) \rangle_p (s/s_0)^z, \quad (15)$$

then the multiplicity ratio is given by

$$R_A \equiv \langle i^z \rangle_A. \quad (16)$$

Furthermore, for the multiplicity distribution in particle-nucleus collisions the model predicts that

$$\Psi_A(z) \cong \Psi_p(z), \quad (17)$$

where

$$\Psi_A(z) = \langle n \rangle_A \frac{\sigma_n}{\sigma_{\text{in}}^A} \quad \text{and} \quad z = \frac{n}{\langle n \rangle_A},$$

and consequently

$$D_A(s) \cong D_p(s_{\text{eff}}) \quad (D_i \cong \sqrt{\langle n^2 \rangle_i - \langle n \rangle_i^2}). \quad (18)$$

Meng Ta-chung [37] suggests that a hadron-nucleus collision is either a *fragmentation process* or a *violent collision*. A violent collision event can be recognized by the observation of a large-transverse momentum particle among the products; and by the fact that the products of this event predominantly populate the central region; and that the multiplicity is relatively high. In fragmentation events the multiplicity is in general low, and the products are mainly found in the projectile and target fragmentation regions.

A comparison with experimental results shows some features in favour of collective models.

For example, it has been observed in several investigations that the scaled multiplicity distributions are in agreement with the Slattery pp-curve, but the function  $\psi(n_s/\langle n_s \rangle)$  may have a weak  $A$ -dependence [6, 19, 38]. As an example of this, results obtained by Jain et al. [38] and Hebert et al. [19] are shown in Figures 15, 16 and 17.

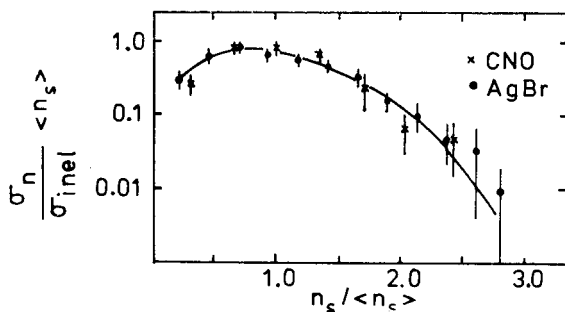


Fig. 15. Slattery pp-curve (solid curve) compared to scaled multiplicity distributions in p-CNO and p-AgBr interactions (Ref. [19])

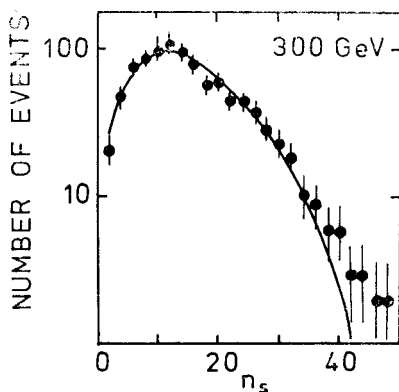


Fig. 16. Comparison of experimental multiplicity distributions in proton-emulsion nucleus interactions at 200 GeV and distributions obtained from KNO scaling (Ref. [38])

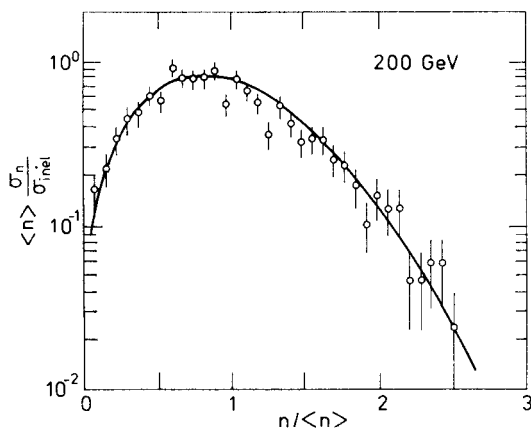


Fig. 17. Comparison of experimental multiplicity distributions in proton emulsion nucleus interactions and multiplicity distribution computed from Slattery curves obtained for each of the three different target components in emulsion (Ref. [19])

Experiments on the production of hadrons and leptons with large transverse momenta at high incident energy and large angles show that the single-particle inclusive cross-sections have a target mass dependence  $A^{\alpha(p_{\perp})}$ , where the exponent  $\alpha(p_{\perp})$  increases with  $p_{\perp}$  and is greater than 1 for  $p_{\perp} \gtrsim 2.5$  GeV ([37] and references therein). One possibility of interpreting these observations is to assume that the incident hadron is acting collectively with target nucleons [1, 36, 37].

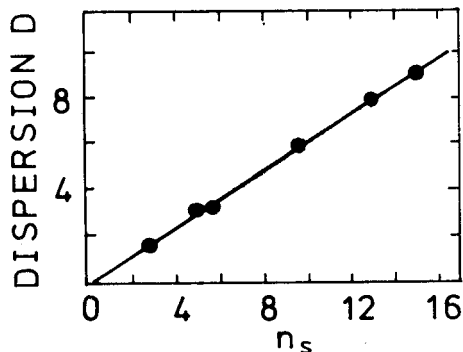


Fig. 18. Dispersion  $D$  as a function of  $n_s$  (Ref. [19])

The ratio  $\langle n_s \rangle / D$  remains constant within the limit of experimental errors. This ratio already appears to have reached a constant value even at an energy of 6 GeV. This is shown in Fig. 18, where the dispersion  $D$  is plotted as a function of shower-particle multiplicity in the energy range  $6.2 \leq E_0 \leq 300$  GeV [19]. A least square fit to the experimental points gives  $D = (0.60 \pm 0.04) \langle n_s \rangle$ . For p-nucleus collisions in (CNO) and (AgBr) at 300 GeV, the value  $\langle n_s \rangle / D$  is found to be close to 2, which is in agreement with the value obtained for pp-collisions at this energy [19]. However, it has been argued by Białas and Czyż [39] that the measurements of the dispersion and of the multiplicity distributions in hadron-nucleus collisions favour the processes of particle production in independent collisions between the incident hadron and target nucleons.

Furthermore, the mean multiplicities and the rapidity distributions predicted from, for example, the Coherent Tube Model are not compatible with the experimental results unless one assumes that there is a large admixture of knock-out protons among the shower-particles.

As was pointed out in the introduction, a determination of the number of recoiling protons among the shower-particles is obviously of great importance for a correct interpretation of the experimental results and for conclusions as to what extent the collective models can reproduce the experimental results.

### 7.3. Independent particle models

In these models the first stage of a hadron-nucleus collision can be considered as a single collision of a hadron with a nucleon. The behaviour of the hadron matter just after the first collision must be determined and different possibilities for this behaviour are discussed

in the independent particle models. One class of models (one-step models) involves those production mechanisms where all the created particles exist within the nucleus. This would produce a multiplicative process that gives shower-particle multiplicities much larger than those observed in hadron-nucleon interactions. From the observed low multiplicities the one-step models can be ruled out.

It is inadequate to suppose that the observed particles actually exist immediately after the first stage of the interaction. In the Energy Flux Cascade Model [32], for example, the created particles emerge from continuous hadronic matter long after the collision is over. In this model the continuous hadronic matter propagating through the target is divided into slices with the rapidity thickness of a single hadron. Thus, from the first

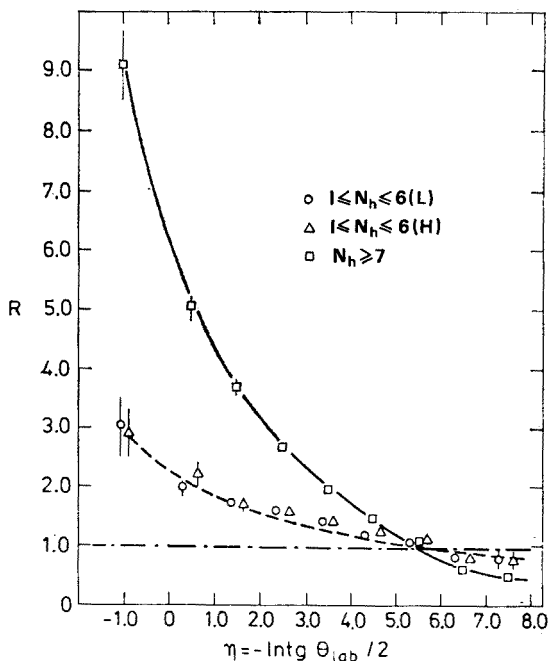


Fig. 19.  $R$  as a function of  $\eta = -\ln \tan \theta/2$  (Ref. [43])

collision one hard and one soft hadron are produced. The hard hadron continues with an energy almost equal to that of the projectile ( $E_0$ ) whereas the soft hadron has a comparatively low energy  $\sim E_0^{1/3}$ . The slices react independently with down stream nucleons as if they were real particles. Each soft hadron produces  $1/3 \langle n_{ch} \rangle$  charged particles in the mean, and the hard hadron produces  $2/3 \langle n_{ch} \rangle$  charged particles. The finite energy corrections to this model were recently estimated by Anderson [40]. In this investigation he found that several slices can be split off during two successive collisions.

Fukushima [41] has recently examined the changes of the rapidity distributions of the slices which react with the target nucleons. The main conclusion to be drawn from his estimation is that  $R$  will be negative for large values of  $\eta$ . Experimentally, this has

been observed in many investigations [5, 15, 42, 43]. As an example,  $R = R(\eta)$ , obtained by the Alma-Ata-Leningrad-Moscow-Tashkent [43] collaboration, is shown in Fig. 19. Similar results are observed in Fig. 14b.

In models suggested by Dar and Vary [35], Fishbane and Trefil [34], and Friedländer et al. [33], the intermediate states are generated by diffractive excitation of the incident proton and the target nucleons. In the first collision, a fast and a slow excited state are produced. The fast one produces new slow excited states during the passage through the nucleus. The slow and fast states decay into  $\frac{1}{2}\langle n_{ch} \rangle$  particles. The multiplicity ratio  $R$  predicted from these models is

$$R = 1 + \eta(\bar{v} - 1) \quad (19)$$

with  $\eta = \frac{1}{2}$  or  $\frac{1}{3} \cdot \eta = \frac{1}{3}$  results from the EFC-model [32].

Andersson and Otterlund [5] have developed a phenomenological model for high energy hadron-nucleus collisions. In this model the multiplicity distributions of shower-particles and heavy prong particles are described as a convolution of a leading particle contribution (LP component, index 0) and one equal and independent contribution (index  $i$ ) from each of the repeated collisions (RC) of the impinging proton and the nucleons inside the nucleus. The total multiplicity of shower-particles,  $\eta_s$ , results as a sum of contributions from the LP-component  $n_0$ , and from the RC-component, produced in  $v-1$  repeated encounters,  $n_i$ ,  $i = 2, \dots, v$ :

$$n_s = n_0 + \sum_{i=2}^v n_i \equiv n_0 + n. \quad (20)$$

The independence assumption implies the following formulas for the mean multiplicity for a given number of collisions  $v$ :

$$\bar{n}_s = \bar{n}_0 + \sum_{i=2}^v \bar{n}_i = \bar{n}_0 + \bar{n}_1(v-1). \quad (21)$$

An operational definition of the LP component is to associate it with the single collision inside the nucleus. Then the RC component corresponds to the excess from the remaining collisions. There are  $(v-1)$  RC-contributions and the multiplicity distribution stemming from each one of them is the same,  $P_{s1}$ . Thus, the  $i$ :th RC-contribution will exhibit itself by  $n_i$  shower-particles with the probability  $P_{s1}(n_i)$ . Then, the combined probability  $P_{RC}(n, v)$  that the RC-component will result in  $n$  shower-particles is constructed as

$$P_{RC}(n, v) = \sum_{n_2 + n_3 + \dots + n_v = n} \prod_{i=2}^v P_{s1}(n_i). \quad (22)$$

The corresponding probability distribution that the LP-component results in  $n_0$  shower-particles is given by  $P_{LP}(n_0)$  so that the total shower-particle distribution for  $v$  collisions is:

$$P_s(n_s, v) = \sum_{n_0 + n = n_s} P_{LP}(n_0) P_{RC}(n, v). \quad (23)$$

In this calculation a negative binomial distribution was used for  $P_{LP}(n_0)$ , and a Poisson distribution for  $P_{s1}(n_i)$ . The differential distribution is described then by the following formula

$$P(n_s) = \sum_{j=1}^2 \alpha_j \sum_{v=1}^{\infty} \pi_j(v) P_s(n_s, v). \quad (24)$$

Here  $\alpha_1$  and  $\alpha_2$  are the probabilities that an event stems from a light (CNO), respectively a heavy (AgBr) nucleus in emulsion. The summation over  $j$  corresponds to the averaging over light and heavy emulsion nuclei.

In Figs 4a and b the experimental results are compared with the predictions from the phenomenological model (Model 3), from the EFC-model ( $\bar{n}_0 = \bar{n}_{ch}$  = mean charged-particle multiplicity in pp-collisions,  $\bar{n}_1 = 0.38 \bar{n}_{ch}$ ) and from the L-model ( $\bar{n}_0 = \bar{n}_{ch}$ ,  $\bar{n}_1 = 0.5 \bar{n}_{\pi}$  = the mean number of pions produced in pp-collisions). In the L-model, the intention was to give  $\bar{n}_0$  the shower-particle multiplicity value obtained in collisions between free protons. The Gottfried parameter  $\eta = 0.5$  was only applied to the multiplicity of created particles ( $n_{\pi}$ ). The comparison shows that the EFC-model and the L-model are not easily compatible with the experimental distributions.

Andersson and Otterlund [44] have also investigated the integral distribution  $\bar{n}_s(u, n_s)$ . This distribution is defined as the total number of tracks (normalized to one event) with an angle smaller than the one characterized by the parameter  $u = \log(\tan \theta)$  in events corresponding to a fixed number of  $n_s$  of shower-particles.

Experimentally, we know that there is a linear relationship between the mean shower-particle multiplicity  $\bar{n}_s(N_h)$  and the heavy prong multiplicity  $\bar{n}_s = \alpha + \beta N_h$  (see Fig. 12a). It turns out that the parameters  $\beta$  and  $\bar{n}_1$  can be related through the number

$$\bar{n}_1 = n_h \beta \quad \text{where} \quad \bar{N}_h(v) = n_h v (v > 1). \quad (25)$$

With  $\bar{n}_0$ , we denote the number of shower-particles produced when  $v = 1$ . In reactions with  $v = 1$ , the mean value of  $\langle N_h \rangle \neq 0$  and equal to  $N_0$ . An approximative value for  $\bar{n}_0$  may be given by the equation

$$\bar{n}_0 = \alpha + \beta N_0. \quad (26)$$

We assume that the angular distribution for a fixed number ( $v$ ) of collisions is given by the formula

$$n(u, v) = n_0(u) + (v-1)n_1(u). \quad (27)$$

In case the relations in Eqs (25) and (26) can be used in a differential way, we know all the quantities in Eq. (27).

$$n_0(u) = \alpha(u) + N_0 \beta(u), \quad (28)$$

$$n_1(u) = n_h \beta(u). \quad (29)$$

Then, the distribution  $\bar{n}_s(u, n_s)$  should be given by the construction

$$\bar{n}_s(u, n_s) = \left[ \sum_v \pi(v) P_s(n_s, v) \right]^{-1} \left( \sum_v \pi(v) n(u, v) P_s(n_s, v) \right) \quad (30)$$

where  $\pi(v)$  is the probability that there will be  $v$  collisions when a proton of energy  $E_0$ ,

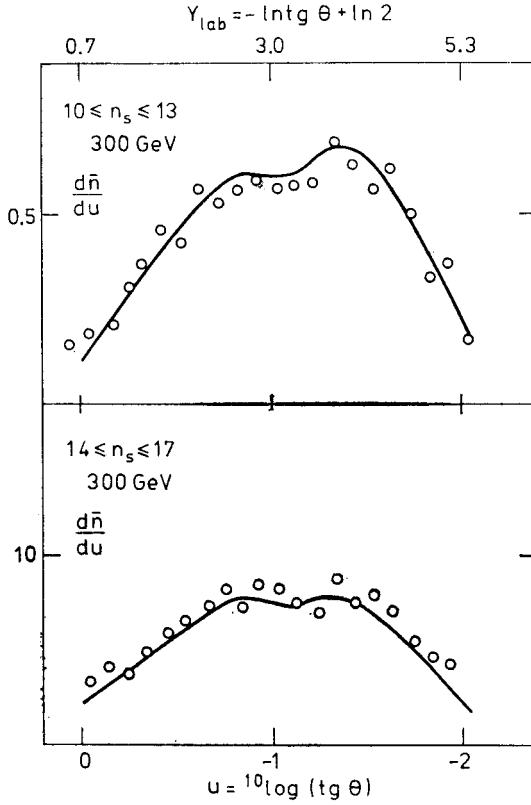


Fig. 20. The differential distribution  $\frac{d\bar{n}_s}{du}$  for  $10 \leq n_s \leq 13$  and  $14 \leq n_s \leq 17$  at 300 GeV [15]. The curves stem from the theoretical prediction Eq. (30) (Ref. [44])

impinging upon emulsion nuclei and the distribution  $P_s$ , gives the probability that given  $v$  collisions, we shall observe exactly  $n_s$  shower-particles. Fig. 20 shows the predictions from these calculations compared with experimental pseudo-rapidity distributions.

### 8. Conclusions

In conclusion the emulsion results can be summarized as follows:

- (i) The ratio of the mean multiplicities in proton-nucleus and proton-proton interactions seems to be energy independent when  $E_0 \gtrsim 60$  GeV.
- (ii) The mean number of heavy prong particles (target fragments) is energy independent.



(iii) The dependence of the mean value of  $n_s$  on  $N_h$  obeys a scaling law

$$\langle n_s(E_0, N_h) \rangle = \langle n_{ch}(E_0) \rangle R(N_h).$$

$R(N_h)$  seems not only to be energy independent but also mass independent at least when  $N_h \ll Z$  (the charge number of the target).

(iv) Topological cross section data in the range 30 — 300 GeV have been found to scale in the variable  $z = n_s / \langle n_s \rangle$  with a scaling function similar to that in pp interactions. The scaling function may have a small dependence on the target mass.

(v) In the projectile fragmentation region the pseudorapidity distribution is similar to that observed in pp reactions. However, there is a small deficit compared to pp distributions. The rapidity distribution in the target fragmentation region does not change with energy. With increasing target mass the excess is observed in the target fragmentation region and in the pionization region.

(vi) Emission of backward particles with  $\beta > 0.7$  increases rapidly with the mass of the target nucleus and they are emitted more abundantly than expected.

(vii) A determination of the number of recoiling protons among the shower particles is of great importance for a correct interpretation of the experimental results and for conclusions as to what extent the suggested theoretical models can reproduce the experimental results.

In preparing this talk I had a great help from my colleagues and many physicists in the field. In particular I wish to thank the participants in the Belgrade-Lund-Nancy-Ottawa-Paris-Rome-Valencia collaboration for use of the commonly scanned material. I would also like to thank B. Andersson and J. Babecki for fruitful discussions. I am grateful to all the authors who send me results relevant to this talk.

## REFERENCES

- [1] Y. Afek et al., Preprint (1976).
- [2] W. Busza, *Proceedings of the VIth International Conference on High Energy Physics and Nuclear Structure*, Sante Fe and Los Alamos, June 1975.
- [3] A. Białas, W. Czyż, *Phys. Lett.* **B51**, 179 (1974).
- [4] S. P. Denisov et al., *Nucl. Phys.* **B61**, 62 (1973); E. L. Berger et al., *Nucl. Phys.* **B77**, 365 (1974); D. Bogert et al., *Phys. Rev. Lett.* **31**, 1271 (1973); D. Fong et al., *Phys. Lett.* **53B**, 290 (1974); Dao et al., *Phys. Rev. Lett.* **29**, 1627 (1972); Chapman et al., *Phys. Rev. Lett.* **29**, 1686 (1972).
- [5] B. Andersson, I. Otterlund, *Nucl. Phys.* **B99**, 425 (1975).
- [6] Alma-Ata-Leningrad-Moscow-Tashkent collaboration, Preprint No 9, Moscow 1974.
- [7] J. R. Florian et al., *Phys. Rev.* **D10**, 783 (1974).
- [8] J. Hebert et al., Barcelona-Batavia-Belgrade-Bucharest-Lund-Lyons-Montreal-Nancy-Ottawa-Paris-Rome-Strasbourg-Valencia collaboration, *Phys. Lett.* **48B**, 467 (1974).
- [9] J. Babecki, Kraków Report No 911/PH (1976).
- [10] E. L. Feinberg, *Phys. Reports* **6C**, No 5 (1972); I. Otterlund et al., Barcelona-Batavia-Belgrade-Bucharest-Lund-Lyons-Montreal-Nancy-Ottawa-Paris-Rome-Strasbourg-Valencia collaboration, *5th Int. Conf. on High-Energy Physics and Nuclear Structure*, Uppsala 1973; A. Gurtu et al., *Phys. Lett.* **50B**, 391 (1974); Alma-Ata-Leningrad-Moscow-Tashkent collaboration, *Sov. J. Nucl. Phys.* **19**, 536 (1974); P. L. Jain et al., *Phys. Rev. Lett.* **34**, 972 (1975); P. R. Vishwanath et al., *Phys. Lett.* **53B**, 479 (1975).

- [11] G. Calucci, R. Jengo, A. Pignotti, *Phys. Rev.* **D10**, 1468 (1974); W. Busza (Ref. [2]).
- [12] H. Winzeler, *Nucl. Phys.* **69**, 661 (1965); H. Meyer et al., *Nuovo Cimento* **28**, 1399 (1963); J. Babecki et al., *Phys. Lett.* **47B**, 269 (1973); K. M. Abdo et al, Preprint JINR, E1-8021 (1974); A. Gurtu et al., (Ref. [10]); J. Hebert et al., (Ref. [8]) private communication; P. L. Jain et al., (Ref. [10]); I. Otterlund, Univ. of Lund Report No LUIP-CR-74-12 (1974); J. Gierula et al., *Acta Phys. Pol.* **B2**, 95 (1971); L. Lohrmann, M. W. Teucher, *Nuovo Cimento* **25**, 957 (1962); S. N. Ganguli et al., (unpublished).
- [13] J. S. Loos et al., Preprint 1975; J. R. Elliot et al., *Phys. Rev. Lett.* **34**, 607 (1975).
- [14] J. Babecki, Kraków Report INP No 887/PH (1975) and No 911/PH (1976).
- [15] Belgrade-Lund-Nancy-Ottawa-Paris-Rome-Valencia collaboration, to be published.
- [16] A. Sheng et al., *Phys. Rev.* **D12**, 1219 (1975). The values  $\langle n_{ch} \rangle_{pn} = 7.84 \pm 0.17$  and  $\langle n_{ch} \rangle = 8.50 \pm 0.12$  (Ref. [17]) give the charged particle multiplicity in proton-nucleon reactions  $\langle n_{ch} \rangle = 8.17 \pm 0.2$ . Using the mean number of slow pions calculated by Calucci et al. [11] we obtain  $\langle n_s \rangle \approx 8.0$ .
- [17] Firestone et al., *Phys. Rev.* **D10**, 2080 (1974).
- [18] J. Babecki et al., private communication.
- [19] J. Hebert et al., Barcelona-Batavia-Belgrade-Bucharest-Lund-Montreal-Nancy-Ottawa-Paris-Rome-Strasbourg-Valencia collaboration, *Proc. of the 14th Int. Cosmic Ray Conf.*, Munich, August (1975).
- [20] B. Andersson, I. Otterlund, *Nucl. Phys.* **B88**, 349 (1975).
- [21] G. Fujioka et al., *J. Phys. Soc. Japan* **39**, 1131 (1975); Hayashino et al., to be published in *Lett. Nuovo Cimento* (1976).
- [22] G.P.S. Occhialini, Meulemans, Vincent, *Nuovo Cimento* **8**, 342 (1951).
- [23] M. Danysz, G. Yekutieli, *Phil. Mag.* **42**, 1183 (1951).
- [24] B. Lindkvist, to be published. The use of wire loaded emulsions in the Bucharest-CERN-Cornell-Lund proton-nucleus experiment was suggested by A. J. Herz, CERN. The grids were manufactured by R. Lorenzi, CERN, using a special equipment developed in the Bucharest-CERN-Cornell-Lund collaboration, private communication.
- [25] J. R. Florian, Preprint, September 1975.
- [26] J. Hebert et al., Barcelona-Batavia-Belgrade-Bucharest-Lund-Lyon-Mc Gill-Nancy-Ottawa-Paris-Quebeck-Rome-Valencia collaboration, *Proceedings of the Vanderbilt Conf. on High Energy Particle Collisions*, Nashville, Tenn., March 1973; *Proceedings of the Fifth International Conference on High Energy Physics and Nuclear Structure*, Uppsala, Sweden, June 1973; I. Otterlund, University of Lund preprint LUIP-CR-74-12 (1974).
- [27] Alma-Ata-Leningrad-Moscow-Tashkent collaboration, *Sov. J. Nucl. Phys.* **19**, 536 (1974).
- [28] F. Białas, W. Czyż, (Ref. [2]); B. N. Kalinkin, Y. L. Schmonin, Preprint JINR, E2-9137 (1975); F. Takagi, *Lett. Nuovo Cimento* **14**, 559 (1975); M. Teranaka, T. Ogata, *Progr. Theor. Phys.* **54**, 1727 (1975); A. Dar et al., (Ref. [1]).
- [29] L. D. Landau, in collected papers of L. D. Landau, Gordon and Breach, N.Y. 1968; S. Z. Belenkij, L. D. Landau, *Nuovo Cimento Suppl.* **III**, Serie X, 15 (1956); G. A. Milekhin, *JETP Soviet Physics* **8**, 682, 829 (1959); S. Z. Belenkij, G. A. Milekhin, *JETP Soviet Physics* **2**, 14 (1956); B. Andersson, preprint Lund University LUTP 76-4 (1976).
- [30] L. Bertocchi, *Proceeding of the VIth International Conference on High Energy Physics and Nuclear Structure*, Santa Fe and Los Alamos 1975 (and references therein).
- [31] M. Miśkiewicz, *Proc. of XI Int. Conf. on Cosmic Rays*, Budapest 1967; *Progress in Elementary Particle and Cosmic Ray Physics* **10**, 128 (1971); J. Babecki (Ref. [9]).
- [32] K. Gottfried, *Proceedings of the Vth International Conference on High Energy Physics and Nuclear Structure*, Uppsala 1973; *Phys. Rev. Lett.* **32**, 957 (1974).
- [33] E. M. Friedlander, *Lett. Nuovo Cimento* **9**, 349 (1974).
- [34] P. M. Fishbane, J. S. Trefil, *Phys. Rev.* **D9**, 168 (1974).
- [35] A. Dar, J. Vary, *Phys. Rev.* **D6**, 2412 (1972).
- [36] S. Fredriksson, Stockholm Royal Institute of Technology, Preprint TRITA-TFY-75-13 (1975).

- [37] Meng Ta-chung, Preprint ITP-SB-76-7 (1976).
- [38] Jain et al., *Phys. Rev. Lett.* **34**, 972 (1975).
- [39] A. Białas, W. Czyż, *Phys. Lett.* **58B**, 325 (1975).
- [40] B. Andersson, *Nucl. Phys.* **B95**, 237 (1975).
- [41] K. Fukushima, Kobe University Preprint, 1976.
- [42] G. Fuijoka, private communication.
- [43] Anzon et al. Alma-Ata-Leningrad-Moscow-Tashkent collaboration, Paper 93, XVII Int. Conf. on HE Phys. London, 1974.
- [44] B. Andersson, I. Otterlund, *Nucl. Phys.* **B102**, 238 (1976).